Advanced Multi-Temperature Heat Pump Model for Industrial Decarbonization: A Realistic Multi-Energy System Optimization Approach

Jan Luca Blaensdorf[*,a,b], Lukas Hoettecke[a], Paul Stursberg[a] and Stefan Niessen[a,b]*

[a] *Foundational Technologies, Siemens AG, Munich/Erlangen, Germany,*
[b] *Technology and Economics of Multimodal Energy Systems, TU Darmstadt, Darmstadt, Germany,*
**Corresponding author: jan-luca.blaensdorf@siemens.com*

Abstract:
Industrial heat decarbonization remains a major challenge particularly for reliable supply of process heating demands at high temperature levels. Breweries represent a particularly interesting case, as their thermal demand is substantial but largely below 200 °C. This makes them suitable candidates for electrification with heat pumps. A new physically grounded representation of heat pumps is presented here. It is integrated into a techno-economic optimization model for a brewery energy system, in order to compare several electrification pathways. These pathways include a single high-temperature heat pump, multiple demand-specific heat pumps, and an integrated multilevel heat pump system with heat-flow optimization across temperature stages. The results show that the best overall performance is achieved by the multilevel heat pump configuration, which systematically reuses intermediate heat flows, resulting in the lowest lifetime total expenditures. The findings highlight that realistic heat pump modelling and temperature-level integration are crucial for identifying viable electrification roadmaps in industrial multi-temperature energy systems. At the same time, economic attractiveness remains highly sensitive to future energy prices, carbon costs, and practical retrofit requirements.

Keywords:
Energy Systems; High Temperature Heat Pumps; Multilevel Heat Pump Systems; Decarbonization.

1. Introduction

The food and beverage (F&B) industry is an energy-intensive industrial sector, with breweries requiring substantial amounts of process heat for steps such as mashing, wort boiling, and pasteurization [1–4]. Because most of this heat is still generated on-site from fossil fuels, industrial heat remains a major lever for decarbonization [5–7]. At the same time, brewery heat demand is typically in the range of 60 to 140 °C and provides a good opportunity for waste heat utilization, making the sector a promising candidate for electrification [8]. Decarbonization strategies for breweries have mainly focused on combinations of renewable electricity generation, storage, electric boilers, heat pumps (HPs), waste heat recovery, and operational optimization [2,3,5,6,9]. In this context, HPs are particularly recognized as a promising technology because they can upgrade low- and medium-temperature heat sources efficiently and thereby reduce both fuel consumption and emissions. However, in many energy system optimization studies, HPs are represented in simplified approaches, e.g., through a fixed coefficient of performance (COP) [6,10–12]. This limitation becomes particularly relevant when considering high-temperature heat pumps (HTHPs) for industrial process heat. HTHPs can supply the temperature levels required in brewery applications, but single-stage systems often face efficiency and reliability challenges at high temperature lifts [13–18]. For this reason, multi-stage configurations such as cascaded and multilevel heat pumps (MLHP) are of particular interest. By splitting the temperature lift across several stages, utilizing optimized refrigerants for each stage, these systems can improve thermodynamic performance for the high temperatures needed in breweries [14,17,19]. Especially in the context of fully electrified industrial multi-temperature energy systems, MLHPs are a promising option because they can simultaneously provide heat at several temperature levels while making use of intermediate stages efficiently. This makes them particularly attractive for brewery processes and other F&B applications with diverse thermal demands [16,19–21]. Against this background, this study investigates how more

physically grounded representations of cascading HTHPs and MLHPs can be integrated into brewery energy systems and what efficiency and decarbonization benefits they may offer.

2. Literature review

Brewery energy systems are conventionally built around centralized gas or oil-fired boilers producing high-pressure steam, distributed to process units, with electrical demand met almost exclusively from the grid [2,4,6,22]. Modern decarbonization pathways move beyond simple boiler replacement toward multi-modal system designs, integrating renewable generation, power-to-heat technologies, and waste heat recovery, typically optimized using Mixed-Integer Linear Programming (MILP) frameworks [5,6,10,22]. Comprehensive multi-modal approaches have demonstrated full decarbonization cost reductions exceeding 30 % compared to simple heat electrification [6].

Within these optimization frameworks, HP modelling is predominantly based on constant COP assumptions, which preserves MILP linearity and reduces computational overhead but neglects the significant dependence of performance on fluctuating source and sink temperatures [6,11,12,23,24]. High-fidelity thermodynamic models exist but are generally confined to experimental settings and are considered computationally intractable for large-scale system design [25,26].

For reaching the medium-to-high temperature levels required in brewery applications, cascade and multilevel architectures are of particular relevance. By connecting multiple refrigerant cycles in series via intermediate heat exchangers, these configurations split a large temperature lift into smaller increments, allowing each stage to operate near its design point with refrigerants suited to its temperature range [14,16,27]. Importantly, serial configurations are not limited to integrated single-body units; multiple conventional HPs installed in series can achieve similar effects, and where intermediate stages directly serve lower-temperature process demands rather than acting solely as thermal bridge, effective energy cascade utilization is realized [14,16]. Through optimized sizing and load distribution across stages, such systems can outperform standalone HTHPs and offer a compelling pathway for industrial electrification at multiple temperature levels. Existing studies typically focus on the energetic optimization of standalone HP units, parallel sequencing strategies, or conventional two-stage cascades designed to meet a single high-temperature delivery point [16,19,21]. However, they seldom model the thermodynamic and operational interactions between internal temperature stages explicitly to satisfy multiple concurrent process demands. This gap motivates the central focus of this work: developing an optimization framework that captures the cross-stage heat flow interactions of MLHP systems and evaluates their techno-economic benefit within a brewery energy system.

3. Methodology

This chapter presents the methodology used to identify optimal technology pathways. A techno-economic model is applied to rapidly determine optimal equipment sizing and tariff selection by minimizing a multi-year objective function. The overall mathematical optimization framework is introduced in Section 3.1, followed by the modeling of HP efficiencies in Section 3.2 and heat flows in Section 3.3. Section 3.4 provides details on the brewery case study used in this work.

3.1. Mathematical optimization model

The model is based upon the optimization framework developed and improved by [6,28,29]. The minimization approach generally is to minimize the total costs of all technologies k

$$\sum_{k \in K} c_k^{TOTEX}, \tag{1}$$

by solving a MILP, where the optimization is restricted by constraints that ensure the physical and technical feasibility of the energy system. The core constraints are given in [28,29].

3.2. Modelling of heat pumps

To model HPs realistically but also efficiently we use the following formulation to approximate their real COP based on their sink and source temperature T_{sink} and T_{source}, e.g., sources in the form of outside

temperature or from available waste heat recovery, and sinks reflecting requirements from process and space heating demands:

$$\mathrm{COP}(T_{\mathrm{sink}}, T_{\mathrm{source}}) = \eta_{\mathrm{quality-grade}} \cdot \eta_{\mathrm{Carnot}} \cdot f_{\mathrm{defrost}} \tag{2}$$

The real-world COP combines a stepwise quality-grade efficiency factor capturing real-world irreversibilities not considered in the simple Carnot efficiency $\eta_{\mathrm{Carnot}} = \frac{T_{\mathrm{sink}}}{T_{\mathrm{sink}} - T_{\mathrm{source}}}$. It also adds a defrost correction factor f_{defrost} that penalizes COP in temperature ranges where frost accumulation is significant.

The quality-grade efficiency factor $\eta_{\mathrm{quality-grade}}$ combines losses in HP components, heat exchangers, and more that are hard to accurately model but are often quite well approximated by a constant factor that has been shown to be mostly dependent on temperature lift [30]. Following approaches described in [30–32] we propose the following model for the quality-grade efficiency factor of a water-to-water HP:

$$\eta_{\mathrm{quality-grade,ww}} = \begin{cases} 0.50 & \text{if} \quad \Delta T < 50\ \mathrm{K} \\ 0.43 & \text{if} \quad 50\ \mathrm{K} < \Delta T \leq 90\ \mathrm{K} \\ 0.36 & \text{if} \quad 90\ \mathrm{K} < \Delta T \leq 130\ \mathrm{K} \\ 0.30 & \text{if} \quad \Delta T > 130\ \mathrm{K} \end{cases} \tag{3}$$

For air-source heat pumps (ASHPs) we apply a systematic downward shift of approximately 0.07 at every tier to account for the less efficient heat exchange of air to water according to [30,31].

The defrosting factor comes from the fact that when an ASHP operates in cold, humid conditions, frost accumulates on the outdoor evaporator coil. This frost layer acts as a thermal insulator, reducing heat transfer from the outdoor air and restricts airflow across the coil, increasing compressor workload [33,34]. This triggers reverse-cycle defrost events, during which the system consumes electricity without delivering useful heat, reducing the seasonal COP [35]. The magnitude of the penalty is strongly temperature- and humidity-dependent. This work focusses on climatic conditions in central Europe. The influence of relative humidity on frost formation and the associated defrost penalty was not accounted for in this study. While relative humidity is known to affect the frequency and duration of defrost cycles, no measured humidity time series was available for the investigated location, and substituting site-specific data with a generic climatological average was considered insufficiently accurate to justify its inclusion. The impact is therefore modelled based solely on the outside temperature using a stepwise correction factor defined as:

$$f_{\mathrm{defrost}}(T) = \begin{cases} 1.00 & \text{if} \quad T > 10\ °C \\ 0.98 & \text{if} \quad 5°C < T \leq 10\ °C \\ 0.90 & \text{if} \quad 0°C < T \leq 5\ °C \\ 0.95 & \text{if} \quad T \leq 0\ °C \end{cases} \tag{4}$$

Laboratory and field studies consistently identify the 0 °C to 5 °C range as the most frost-critical operating band, where coil temperatures readily fall below freezing while the ambient air still carries sufficient moisture to sustain rapid frost growth [33,34]. At temperatures below 0 °C, the absolute humidity of the ambient air decreases substantially, reducing the rate of frost deposition and the frequency of defrost events, such that the integrated seasonal penalty is smaller than in the 0 – 5 °C band [35]. Above approximately 10°C, the outdoor coil surface temperature remains above freezing under normal operating conditions and no frost forms, so no defrost penalty applies. For temperature lifts greater than 60 K we apply the defrosting penalties twice to account for the likely higher ice build-up when lifting the already low source temperature to even higher sink temperatures.

This study focuses on industrial sites with typical demands of several MW, where HPs are generally installed in multiple units. Since frequency converters offer stable efficiencies across a broad operating range, this work neglects part-load capabilities, following the approach of [29].

3.3. Modelling of heating demands

Prior work on industrial energy system optimization has largely treated heating demands as purely energetic quantities, associating each demand with a fixed, constant temperature throughout the year [6,36,37]. As discussed in Section 2, this implication can obscure important interactions between temperature levels, particularly in multi-temperature systems where several demands with differing requirements share a common

distribution infrastructure. When all demands on a shared heating system must be served at the temperature of the highest-temperature consumer, the entire system operates at an unnecessarily elevated sink temperature, reducing efficiency for all lower-temperature demands and potentially misrepresenting the true benefit of demand-side measures such as insulation upgrades or heat emitter replacement. Capturing these effects requires that each demand be associated with its own temperature profile, and that the supply temperature itself be modelled realistically.

For process heating demands with fixed temperature requirements, the sink temperature of the HP is directly determined by the process specification. For space heating and similar demands where the required supply temperature varies with ambient conditions, the required heat flow temperature T_{flow} is computed as a function of the desired room temperature T_{room}, the current outside temperature T_{outside}, and a building-specific factor k capturing the combined effect of insulation quality and heat emitter sizing, following the simplified heating curve formulation according to EN 12831, EN 442 and related empirical research [38]:

$$T_{\mathrm{flow}} = T_{\mathrm{room}} + k \cdot (T_{\mathrm{room}} - T_{\mathrm{outside}}) \tag{5}$$

Rather than prescribing a fixed heating infrastructure topology, the model is given the freedom to choose which combination of supply temperature levels to install. In practice, this means the optimizer can decide whether to generate heat at the highest required process temperature and distribute it to lower-temperature demands via vents or heat exchangers, or whether to install dedicated HP stages that deliver heat directly at each, possibly time-variant process temperature level. Each of these configurations carries a different balance of capital expenditures (CAPEX), determined by the number, size, and type of HP units installed, and operating expenditures (OPEX), determined by the efficiency at which each unit operates given its specific temperature lift. The model therefore implicitly compares the cost of additional heating infrastructure at intermediate temperature levels against the lifetime operating savings that more targeted heat delivery enables through higher COPs.

In principle, this framework allows HP inputs and outputs to be defined at any temperature level, not only at the discrete process temperatures. In practice, however, restricting HP connection points to the actual process temperature levels is a well-justified simplification for early-stage system design [11,36,37], where the relevant temperature requirements are known and intermediate levels would add computational complexity without a commensurate gain in planning accuracy. Moreover, with many closely spaced temperature options, solutions can become sensitive to small variations in boundary conditions, reducing robustness. The temperature levels in this study are given by the brewery case study introduced in Section 3.4, which already provides the optimizer with substantial structural freedom while remaining tractable and interpretable. Exploring finer or adaptive temperature discretization remains a valuable direction for future work.

3.4. Brewery case study

The general beer production process includes multiple steps and is well described in [6].

The system modeled for this case study uses data from a real brewery. The existing system is schematically shown in Figure 1. The waste heat source from wort cooling that is not used in the *business-as-usual (BAU)* scenario can be fed into a booster HP for optimized scenarios. The system addresses five distinct process demands: 130 °C steam, 100 °C and 80 °C hot water, and wort cooling. Additionally, room heating (RT) is provided with a time-variable flow temperature, determined by Eq. (5) using $k = 1.5$, corresponding to relatively poor insulation and comparatively small radiators relative to room size, which would fit to a room temperature heating system for a large industrial facility. Additional electricity demand is supplied by the public electric grid. The annual demands for process heating, cooling, and electricity are given in the Appendix (Table A.1). The installed capacities of the different assets are given in Table A.2.

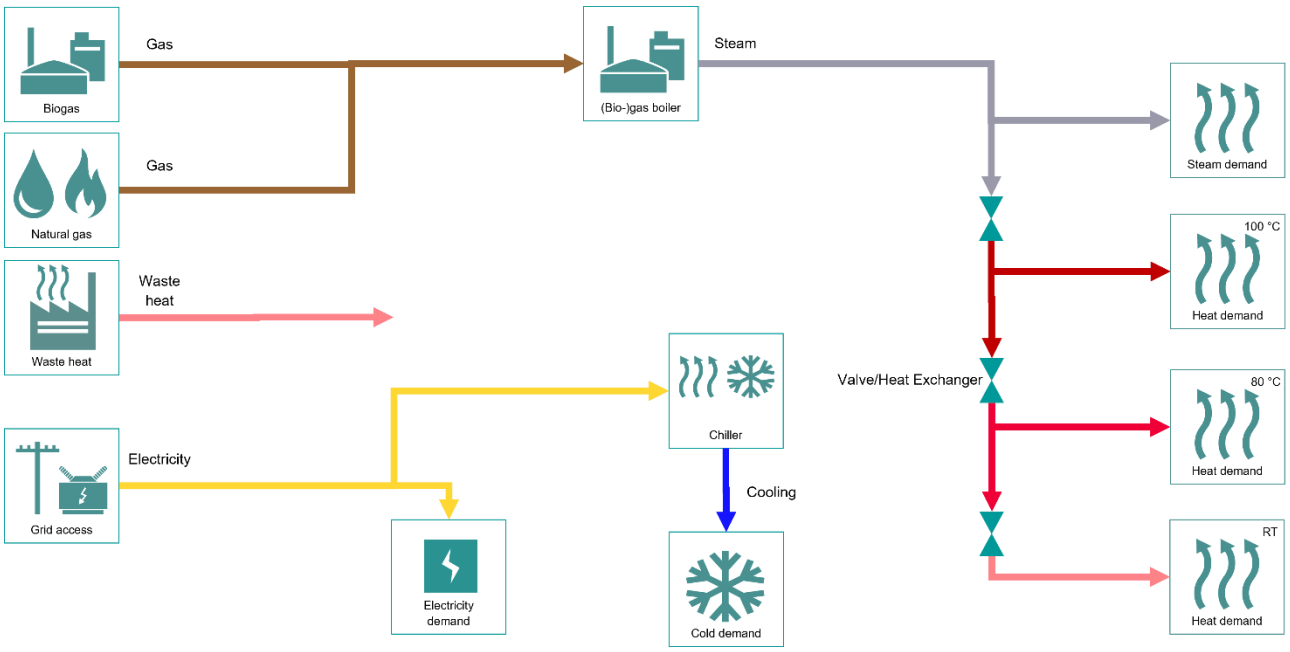

Figure 1. *Simplified energy flow diagram for the BAU scenario. Biogas and natural gas are burned in boiler systems to provide steam at 130 °C that is then subsequently cooled to deliver heat to different process demand temperatures. Electricity from the grid is used in a chiller to provide the cooling demand and to supply supplementary electricity demand. Waste heat is not used.*

The room for improvements includes different electrified scenarios with photovoltaic (PV) systems and lithium-ion batteries. Additionally, a steam, RT hot water, and chilled water storage can be installed. Depending on the different scenarios, HPs of different configurations can be installed, from ASHPs to booster HPs at varying temperature lifts. Installation prices and unit sizes for the installable assets are given in Table A.3. Electricity prices are set to the German spot market prices of 2025, gas prices to 6.7 ct/kWh [39], biogas is extracted from the brewer's spent grain (BSG) and has therefore no cost associated with it. All lifetimes are set to 20 years. An interest rate of 7 % is used. For temperature and PV generation time series, standardized time series for central Europe are used.

As shown in Section 2, there are numerous ways to optimize a brewery's energy system. This paper focuses on the electrification of heat supply. In that respect, four scenarios are compared that are schematically shown in Figure 2. The *BAU* scenario's heat flow is described in Fig. 2.a. A straightforward retrofit in which the gas and biogas boilers of the *BAU* scenario are replaced by a HTHP for a full electrification is shown in Fig. 2.b. This approach follows a one-by-one replacement approach with considerable low planning efforts. This is compared with an alternative configuration that installs four separate HPs (Fig. 2.c), each matched to a specific process temperature level. Finally, an application of heat-flow optimization to MLHP systems, shown in Fig. 2.d, is investigated.

4. Results

As a solver for the optimization problem, Gurobi Optimizer version 10.0.1 was used on a machine with an Intel(R) Xeon(R) Gold 6240R CPU @ 2.40GHz with 24 physical cores, 48 logical processors, using up to 3 threads. The MIP gap was set to 0.1 %.

Section 4.1 evaluates the straightforward retrofit of the *BAU* scenario with an ASHP steam in the *One HTHP* scenario for a full electrification. This is also compared to the *Multiple HP* scenario. Section 4.2 investigates the *MLHP* system under varying parameter assumptions. Finally, Section 4.3 compares the different approaches, discusses their practical realism, and outlines implications for real-world deployment and future developments.

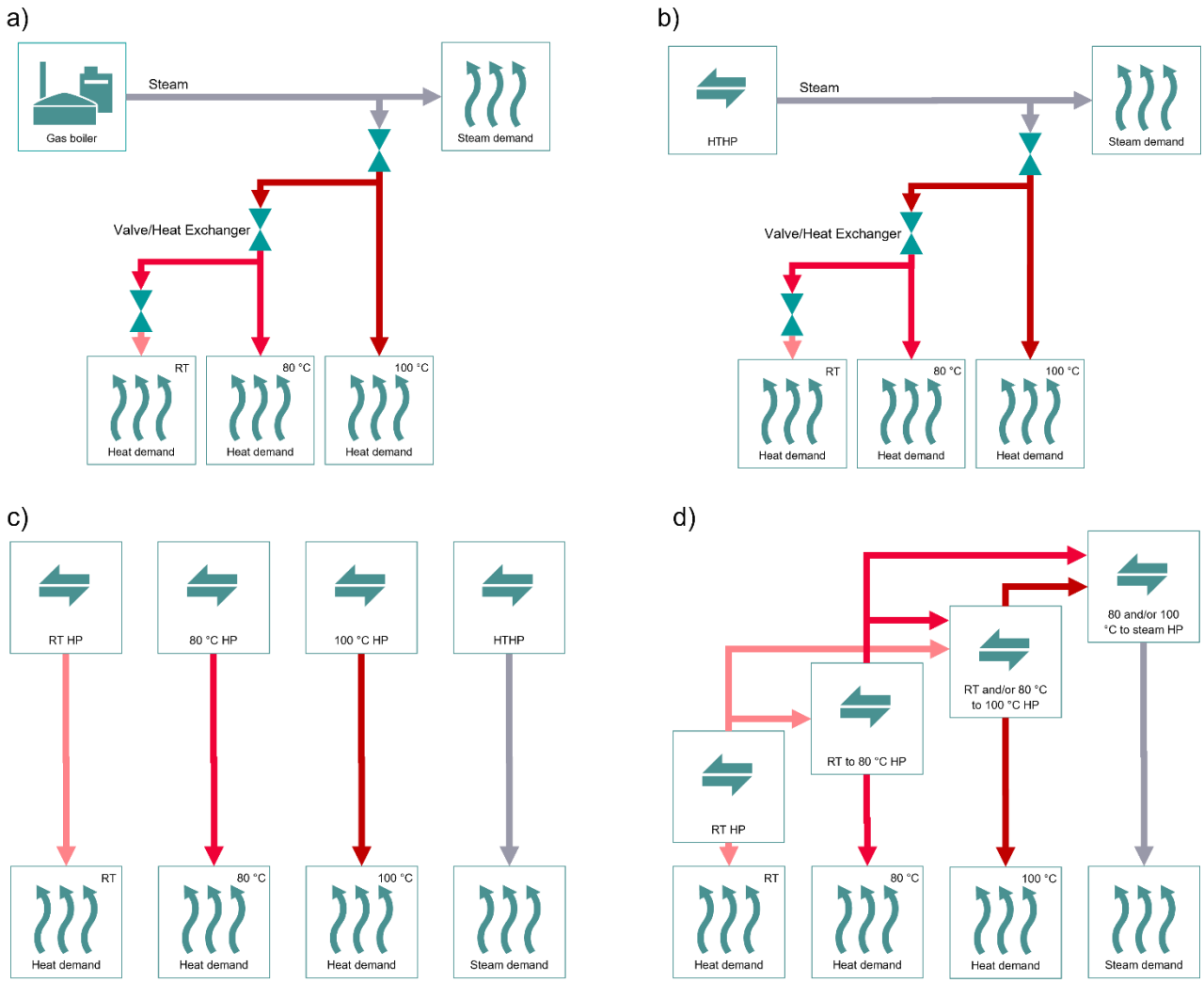

Figure 2. *Simplified heating diagrams for the four different scenarios: a) BAU, b) One HTHP, c) Multiple HP, d) MLHP. The color of the arrows denotes the corresponding temperature of the heat flow. Scenario a) and b) show heat generators producing steam that is then iteratively cooled to the other process temperatures. Scenario c) has ASHPs delivering heat at exactly the temperature needed for each process and scenario d) shows the setup of the cascading MLHP system where the heat flow for each heat demand is used as input for booster HPs to produce higher temperatures. Waste heat is not shown for simplification but flows into a booster HP for RT production. RT HP can be installed either as a single system with extra compression chiller or as a dual-mode HP.*

4.1. One-by-one retrofit vs. process-specific heat supply

Compared with the *BAU* scenario, replacing the gas boiler with a single HTHP (scenario *b* in Fig. 2) results in a substantial increase in both capital and operating expenditures. Total CAPEX amount to 20.59 M€, of which 15 M€ are attributable to the ASHP steam, while the remainder is associated with PV investments and a small thermal storage contribution. In contrast, as a simplification we assume the *BAU* scenario requires no new capital investment in the reference period. Annual OPEX increase from 3.37 M€ in the *BAU* case to 4.44 M€ in the *One HTHP* scenario. The increase in CAPEX is readily explained by the investment required for new equipment, whereas the *BAU* case continues operation of the existing gas boiler infrastructure. The higher OPEX in the *One HTHP* scenario is less obvious at first glance. While the ASHP steam performs efficiently under summer conditions, the model indicates that its winter performance is comparable to that of a gas or electric boiler. This is primarily due to significant defrosting penalties associated with large temperature lifts under low ambient air temperatures. The main economic disadvantage of the *One HTHP* scenario, however, arises from the current energy price structure: natural gas remains considerably cheaper per kilowatt-hour than electricity. Under average spot-market conditions, an electrified heating system would therefore need to achieve roughly three times higher efficiency to attain operating costs comparable to those of the gas-based system. This result is, however, sensitive to assumptions regarding electricity prices, gas prices, and carbon

costs. In particular, rising CO_2 prices and continued geopolitical uncertainty may significantly alter the long-term economic comparison. From an implementation perspective, the *One HTHP* scenario represents a relatively simple replacement of the existing gas boiler and therefore serves as a useful reference case for the electrification of the system. Nevertheless, under the present price assumptions, it does not appear to be an economically attractive option.

Compared with the baseline configuration in the *One HTHP* scenario, the *Multiple HP* scenario (scenario *c* in Fig. 2) considers the deployment of multiple individual HPs that are each matched directly to the specific process temperature levels. This arrangement allows heat to be supplied closer to the required temperature, thereby improving overall system efficiency. In the *One HTHP* scenario, a large fraction of the heat demand is supplied by generating steam with a single ASHP steam and subsequently cascading this heat to lower-temperature processes. According to the model, steam generation via the HTHP operates at a COP that is approximately 2 to 2.4 times lower than that of the ASHP RT. As a result, using high-grade heat for lower-temperature demands introduces avoidable thermodynamic losses, and exergy destruction. These efficiency gains in the *Multiple HP* scenario require additional investment. In addition to an ASHP steam, albeit smaller as it is only dependent on the actual steam demand, the system also includes HPs for supplying heat at 100 °C, 80 °C, and RT-temperature level. Yet, CAPEX decrease by approximately 15 % relative to the *One HTHP* scenario, as can be seen in Fig. 3. As the ASHP steam has a very high electricity consumption, investing heavily in PV has higher benefits for the *One HTHP* scenario (5.54 M€) than for the *Multiple HP* scenario (3.17 M€). Also, the demand-specific sizing of the individual HPs seems to already lead to lower investment costs. These investments remain dominated by the ASHP steam, which accounts for 7.5 M€, followed by the ASHP 80 °C with 3 M€, and the ASHP 100 °C with 2.5 M€. The ASHP 100 °C is more expensive than the ASHP 80 °C but as the demand for 80 °C is on average 50 % higher than for 100 °C demand, this leads to higher CAPEX for this asset. In addition to the moderate decrease in CAPEX, the improved temperature-level matching substantially reduces annual operating costs. The modeled OPEX in the *Multiple HP* scenario are only 60 % of those of the *One HTHP* scenario. Assuming an asset lifetime of 20 years, this, in combination with the CAPEX savings, corresponds to cumulative net savings of up to 38.5 M€ relative to the *One HTHP* scenario. Under the assumptions of this study, the *Multiple HP* scenario is therefore economically preferable to *the One HTHP* scenario, provided that its implementation is technically and spatially feasible. However, relative to the *BAU* scenario, the *Multiple HP* scenario still does not constitute a clearly cost-efficient retrofit, as its lower CAPEX and even lower OPEX are not sufficient to achieve a payback period of less than 20 years.

Both approaches largely treat the HPs as standalone utilities that simply meet each temperature demand, without explicitly optimizing heat flows between process levels. In the next section, we therefore explore how a MLHP system can be coupled through heat-flow optimization to recover and reuse heat across steps and further improve overall performance.

4.2. Heat flow optimization

As discussed, it is often advantageous to use heat from one temperature stage as the source for a subsequent HP cycle in order to reach higher temperature levels more efficiently. Although this cascading principle is inherent to HTHPs, previous system configurations do not systematically utilize intermediate temperature levels to directly serve process demands at those same levels. In contrast, the *MLHP* configuration scenario (scenario *d* in Fig. 2) incrementally raises the temperature from ambient conditions to steam generation through several coordinated HP stages, while recovering and reusing intermediate heat flows wherever possible.

This configuration results in an estimated reduction of 4.54 M€ in total expenditures over the system lifetime relative to the *Multiple HP* scenario. Although the initial CAPEX of the MLHP scenario are approximately 1.5 % higher than those of the *Multiple HP* scenario, the lower operating costs more than compensate for this increase. Specifically, annual OPEX are reduced by 0.24 M€ compared with the *Multiple HP* scenario, such that the additional investment is already recovered after one year. Relative to the *BAU* scenario, however, the *MLHP* scenario remains only marginally attractive from a purely economic perspective. The modeled payback period is 18.8 years, which is close to the assumed lifetime of the installed assets and therefore implies a comparatively high investment risk. Under the assumptions applied here, cumulative savings of approximately 1.07 M€ could still be achieved over 20 years while simultaneously enabling full site electrification. Compared

with the simple single ASHP steam electrification strategy of the *One HTHP* scenario, the *MLHP* scenario reduces lifetime total expenditures by almost 40 %. The different scenario's CAPEX, OPEX, and savings compared to the *BAU* scenario are shown in Table 1.

Table 1. *Comparison of scenario's initial CAPEX, annual OPEX, and total cost savings after 20 years compared to the BAU scenario.*

Scenario	CAPEX [M€]	OPEX [M€/a]	Savings compared to BAU [M€]
BAU	0	3.37	0
One HTHP	20.59	4.44	-41.99
Multiple HP	17.47	2.67	-3.47
MLHP system	17.73	2.43	1.07

In Fig. 3 it can be seen that the largest investment items in the *MLHP* scenario are the ASHP supplying RT heat, followed by the booster HP for 80 °C water and the PV system. This differs from the *Multiple HP* scenario, in which the steam-generating HP represents the dominant cost component. In the *MLHP* scenario, the economic focus shifts toward the first stage of the MLHP chain, which supplies RT heat not only for the corresponding process demand but also as the thermal basis for subsequent temperature lifts in downstream process stages. For this reason, the booster HP waste heat to RT is sized to maximize the use of the waste heat at all times, as this stage operates with the highest efficiency and can be utilized continuously due to the consistently high demand at and above this temperature level. This stands in contrast to the *Multiple HP* scenario, where the installed size of the booster HP waste heat to RT is 25 % smaller than in the *MLHP* scenario as the full capacity of the time-variant waste heat is not needed.

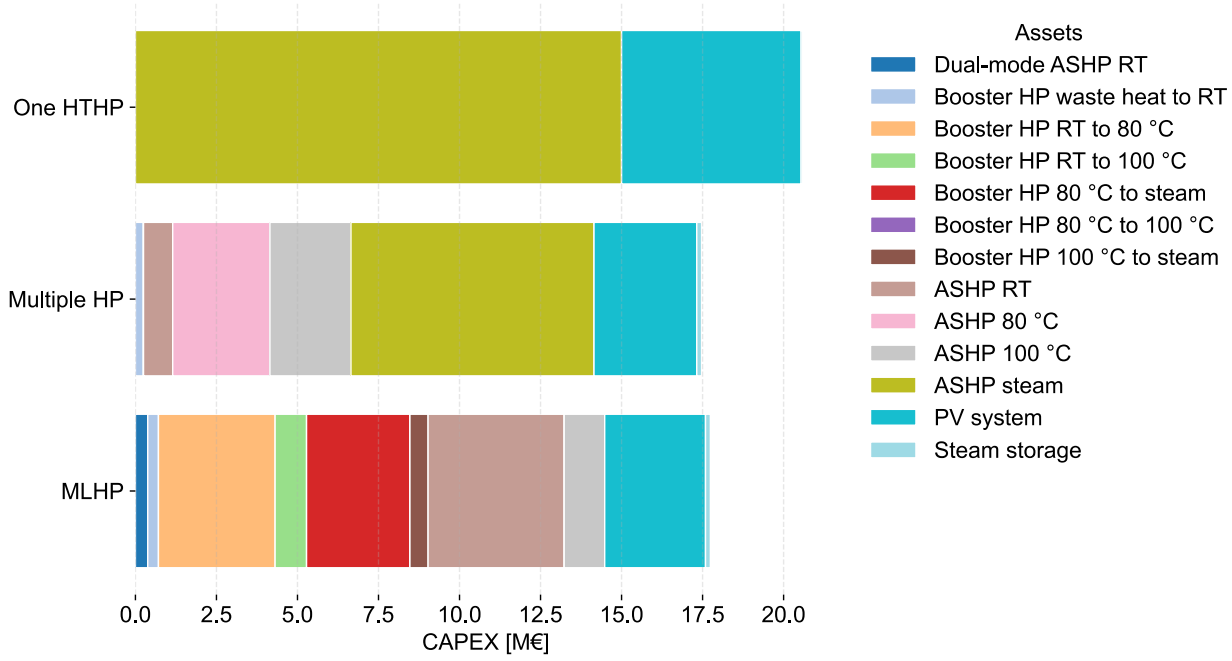

Figure 3. *CAPEX for the three different electrification scenarios broken down by assets.*

4.3. Discussion

The ongoing decarbonization and electrification of industrial manufacturing require new technical concepts for process heat supply. The results of this study indicate that simple electrification through a single HTHP, or similarly through an electric boiler, would lead to substantially higher costs than the current BAU configuration. In contrast, more specialized configurations employing dedicated HPs for individual process temperature levels can significantly reduce operating expenditures, although they remain more expensive than the *BAU* scenario under the present assumptions. The analysis further shows that an intelligently integrated MLHP system can already achieve slight cost savings relative to *BAU* while remaining markedly more economical than the simple *One HTHP* electrification approach. At the same time, several practical constraints may limit

the direct applicability of such a system in real industrial settings. A future research direction may be to refine investment estimation methods accounting for construction and retrofitting measures to integrate a MLHP into existing supply systems. In addition, industrial processes that depend on highly reliable heat supply at precise temperature levels and specific times may require greater system redundancy than a complex MLHP configuration can inherently provide. This could necessitate additional backup capacity and control infrastructure, which would further reduce economic attractiveness. For this reason, the results presented here should not be interpreted as an immediate implementation recommendation. Rather, they are intended to illustrate and compare alternative electrification pathways based on HP technologies in order to support informed long-term decision-making.

The economic assessment is also highly sensitive to future energy price developments. If natural gas prices increase due to stricter CO_2 regulation, higher carbon prices, or geopolitical disruptions, the economic attractiveness of electrified heat supply options would improve considerably. For example, assuming a gas price of 15 ct/kWh, which represents a high but not implausible case according to [40,41], even a simple replacement of the gas boiler with an ASHP steam becomes economically viable. Under such conditions, the MLHP scenario would yield even greater savings. These additional savings could help offset the higher real-world costs associated with retrofit measures, backup systems, and other implementation requirements necessary for industrial deployment.

5. Conclusion & Outlook

This study shows that brewery heat supply can be substantially decarbonized through electrification with HPs. However, the system design choice strongly affects techno-economic performance. A simple replacement of the main gas boiler by a single HTHP is not economically attractive under the assumed energy prices, whereas an integrated assessment including decentralized HPs significantly improve efficiency and reduce lifetime costs. Among the analyzed options, the integrated MLHP system performs best, as it makes better use of intermediate temperature levels and can profit from its increased flexibility while enabling full electrification.

At the same time, the results highlight that economic viability remains sensitive to boundary conditions such as electricity and gas prices, carbon costs, and retrofit complexity. Future work should therefore focus on more detailed site-specific integration studies, including practical implementation constraints, redundancy requirements, and dynamic operation under real process conditions. In addition, finer temperature discretization, more detailed part-load modelling, and the inclusion of forecasting models for loads and multi-market prices could further improve the robustness of the assessment.

Acknowledgments

We would like to thank Johannes Lipka, Peter van Hasselt, Martin Kautz, Florian Reissner, and Christian Lindner for their technical support and their immense practical knowledge about breweries, heat pumps and complex energy systems.

Appendix A

Table A.1. *Annual demands for different processes.*

Process	Maximum [MW]	Average [MW]	Energy Demand [GWh]
Steam demand	7.5	1.24	10.8
100 °C demand	1.7	0.93	8.15
80 °C demand	2.55	1.40	12.2
RT demand	2.8	0.98	8.58
Cooling demand	0.2	0.2	1.75
Electricity demand	0.1	0.1	0.88

Table A.2. *Installed capacities of BAU scenario assets.*

Asset	Installation [MW]
Gas Boiler	12.5
Biogas boiler	0.86
Compression chiller	0.2
Valve steam to 100 °C	10
Valve 100 to 80 °C	8.5
Valve 80 °C to RT	7

Table A.3. *Investment prices and unit sizes of installable assets of the electrification scenarios.*

Asset	Invest [€/kW]	Unit size [kW]
Dual-mode ASHP RT	750	500
Booster HP waste heat to RT	145	250
Booster HP RT to 80 °C	600	500
Booster HP RT to 100 °C	650	500
Booster HP 80 °C to steam	750	250
Booster HP 80 °C to 100 °C	500	250
Booster HP 100 °C to steam	750	250
ASHP RT	600	500
ASHP 80 °C	1000	500
ASHP 100 °C	1250	500
ASHP steam	1500	500
PV system	600	-
Li-ion battery	150 + 400 €/kWh	-
Chilled water storage	20 €/kWh	-
Steam storage	30 €/kWh	-
RT water storage	18.3 €/kWh	-

Nomenclature

Abbreviations

F&B	food & beverage	OPEX	operational expenditures
HP	heat pump	ASHP	air-source heat pump
COP	coefficient of performance	PLR	part-load ratio
MILP	mixed-integer linear programming	RT	flow temperature for room temperature
HTHP	high-temperature heat pump	BSG	brewer's spent grain
MLHP	multilevel heat pump	BAU	business-as-usual
CAPEX	capital expenditures	PV	photovoltaic

Parameters

c	costs	t	time
η	efficiency		

References

[1] Improving energy efficiency in the food and beverage industry. ABB Motion; 2021.

[2] Zhang R, Duyar M, Foulkes L, Berrow J, Short M. Multi-objective optimisation for microbrewery retrofitting. Comput Aided Chem Eng 2023;52:197–202. https://doi.org/10.1016/B978-0-443-15274-0.50032-9.

[3] Kusakana K. Optimal energy management of a grid-connected dual-tracking photovoltaic system with battery storage: Case of a microbrewery under demand response. Energy 2020;212:118782. https://doi.org/10.1016/j.energy.2020.118782.

[4] Decarbonizing process heat in the food and beverage sector with thermal energy storage: a path forward for breweries, coffee, and oilseed industries. Food Drink Netw UK n.d.

[5] Schagon V, Murali R, Zhang R, Duyar M, Short M. An MINLP-based decision-making tool to help microbreweries improve energy efficiency and reduce carbon footprint through retrofits. Digit Chem Eng 2024;13:100189. https://doi.org/10.1016/j.dche.2024.100189.

[6] Lipka JB, Hottecke L, Stursberg P, Metzger M, Heger HJ, Niessen S. Optimal energy system design for brewing site decarbonization via electrification, Paris, France: 2025.

[7] Putz M, Cherkaskyy M, Fanghänel C, Esche A, Schlegel A. Energieeffizienzpotenzial in der Planung am Beispiel der Brauerei-Industrie. Chemnitz, Dresden, Augsburg Und Zittau: Fraunhofer-Institut für Werkzeugmaschinen und Umformtechnik IWU; n.d.
[8] Rehfeldt M, Bussmann S, Fleiter T. Direct electrification of industrial process heat. An assessment of technologies, potentials and future prospects for the EU. Study on behalf of Agora Industry. Fraunhofer ISI; 2024.
[9] Pino A, Lucena FJP, Macho JG. Economic Analysis for Solar Energy Integration in a Microbrewery. 2019 Int. Conf. Smart Energy Syst. Technol. SEST, Porto, Portugal: IEEE; 2019, p. 1–6. https://doi.org/10.1109/SEST.2019.8849128.
[10] Hoettecke L, Schuetz T, Thiem S, Niessen S. Technology pathways for industrial cogeneration systems: Optimal investment planning considering long-term trends. Appl Energy 2022;324:119675. https://doi.org/10.1016/j.apenergy.2022.119675.
[11] Aguilera JJ, Padullés R, Meesenburg W, Markussen WB, Zühlsdorf B, Elmegaard B. Operation optimization in large-scale heat pump systems: A scheduling framework integrating digital twin modelling, demand forecasting, and MILP. Appl Energy 2024;376:124259. https://doi.org/10.1016/j.apenergy.2024.124259.
[12] Pieper H, Ommen T, Kjær Jensen J, Elmegaard B, Brix Markussen W. Comparison of COP estimation methods for large-scale heat pumps used in energy planning. Energy 2020;205:117994. https://doi.org/10.1016/j.energy.2020.117994.
[13] Kabat N, Jende E, Yücel FC, Stathopoulos P. Thermodynamic analysis of a novel high-temperature heat pump cycle with inter cooled compression and reheated expansion based on the reversed Brayton cycle. Int J Sustain Energy 2025;44:2515452. https://doi.org/10.1080/14786451.2025.2515452.
[14] Wu J, Yang L, Zhang C. High-temperature heat pumps: key technologies and industrial applications toward carbon–neutral process heating. Carbon Neutral Syst 2025;1:21. https://doi.org/10.1007/s44438-025-00021-z.
[15] Zühlsdorf. Annex 58 High-Temperature Heat Pumps Final Report. Heat Pump Center; 2024. https://doi.org/10.23697/2QXE-AV87.
[16] Badran E. B, Mota-Babiloni A, Ghanbarpour M, Khodabandeh R. Theoretical study of a multilevel heat pump for multi-source heating., Italy: International Institute of Refrigeration (IIR); 2021. https://doi.org/10.18462/IIR.TPTPR.2021.2206.
[17] Lu Z, Yao Y, Liu G, Ma W, Gong Y. Thermodynamic and Economic Analysis of a High Temperature Cascade Heat Pump System for Steam Generation. Processes 2022;10:1862. https://doi.org/10.3390/pr10091862.
[18] Yu H, Zhao Z. Research on High Temperature Cascade Heat Pump System for Vapor Production Employing Scroll Compressors and Multi-stage Preheat Cycle. World J Appl Phys 2025;10:78–84. https://doi.org/10.11648/j.wjap.20251004.11.
[19] Arpagaus C, Bless F, Schiffmann J, Bertsch SS. Multi-temperature heat pumps: A literature review. Int J Refrig 2016;69:437–65. https://doi.org/10.1016/j.ijrefrig.2016.05.014.
[20] Jung HW, Kang H, Chung H, Ahn JH, Kim Y. Performance optimization of a cascade multi-functional heat pump in various operation modes. Int J Refrig 2014;42:57–68. https://doi.org/10.1016/j.ijrefrig.2014.03.004.
[21] Urrutia LZ, Pascual JF, Sterling R. Heuristic Mathematical Optimization of Heat Pumps in Cascade to Reduce Energy Consumption n.d.
[22] Lipka JB, Höttecke L, Stursberg P, Metzger M, Heger HJ, Niessen S. Including batch scheduling flexibility in industrial energy system design and dispatch optimization: A case study of a brewery. Energy 2026;346:140295. https://doi.org/10.1016/j.energy.2026.140295.
[23] Hoettecke L, Thiem S, Schäfer J, Niessen S. Resilience optimization of multi-modal energy supply systems: Case study in German metal industry. Comput Chem Eng 2022;162:107824. https://doi.org/10.1016/j.compchemeng.2022.107824.
[24] Fink J, Van Leeuwen RP, Hurink JL, Smit GJM. Linear programming control of a group of heat pumps. Energy Sustain Soc 2015;5:33. https://doi.org/10.1186/s13705-015-0061-9.
[25] Gabrielli P, Sansavini G, Singh S, Garcia LS, Jacquemoud E, Jenny P. Off-Design Modeling and Operational Optimization of Trans-Critical Carbon Dioxide Heat Pumps. J Eng Gas Turbines Power 2022;144:101004. https://doi.org/10.1115/1.4055233.
[26] Wang D, Li X, Marquant J, Carmeliet J, Orehounig K. Advancing the Thermal Network Representation for the Optimal Design of Distributed Multi-Energy Systems. Front Energy Res 2021;9:668124. https://doi.org/10.3389/fenrg.2021.668124.
[27] Wang W, Li Y, Hu B. Real-time efficiency optimization of a cascade heat pump system via multivariable extremum seeking. Appl Therm Eng 2020;176:115399. https://doi.org/10.1016/j.applthermaleng.2020.115399.
[28] Thiem SM. Multi-modal on-site energy systems. Doctoral thesis. Technical University Munich, 2017.
[29] Höttecke L. Sustainable Design of Industrial Energy Supply Systems. Doctoral thesis. Technical University Darmstadt, 2023.
[30] Ruhnau O, Hirth L, Praktiknjo A. Time series of heat demand and heat pump efficiency for energy system modeling. Sci Data 2019;6:189. https://doi.org/10.1038/s41597-019-0199-y.
[31] Chua KJ, Chou SK, Yang WM. Advances in heat pump systems: A review. Appl Energy 2010;87:3611–24. https://doi.org/10.1016/j.apenergy.2010.06.014.
[32] Ommen T, Markussen WB, Elmegaard B. Heat pumps in combined heat and power systems. Energy 2014;76:989–1000. https://doi.org/10.1016/j.energy.2014.09.016.
[33] Dong J, Deng S, Jiang Y, Xia L, Yao Y. An experimental study on defrosting heat supplies and energy consumptions during a reverse cycle defrost operation for an air source heat pump. Appl Therm Eng 2012;37:380–7. https://doi.org/10.1016/j.applthermaleng.2011.11.052.
[34] Qu M, Xia L, Deng S, Jiang Y. An experimental investigation on reverse-cycle defrosting performance for an air source heat pump using an electronic expansion valve. Appl Energy 2012;97:327–33. https://doi.org/10.1016/j.apenergy.2011.11.057.
[35] Bagarella G, Lazzarin R, Noro M. Annual simulation, energy and economic analysis of hybrid heat pump systems for residential buildings. Appl Therm Eng 2016;99:485–94. https://doi.org/10.1016/j.applthermaleng.2016.01.089.
[36] Krützfeldt H, Vering C, Mehrfeld P, Müller D. MILP design optimization of heat pump systems in German residential buildings. Energy Build 2021;249:111204. https://doi.org/10.1016/j.enbuild.2021.111204.
[37] Moretti L, Manzolini G, Martelli E. A MILP Model for the Operational Planning of Multi-Energy Systems Accounting for variable Delivery/Return Temperatures and Non-Isothermal Mixing in Headers. Comput. Aided Chem. Eng., vol. 48, Elsevier; 2020, p. 1501–6. https://doi.org/10.1016/B978-0-12-823377-1.50251-2.
[38] Staffell I, Pfenninger S, Johnson N. A global model of hourly space heating and cooling demand at multiple spatial scales. Nat Energy 2023;8:1328–44. https://doi.org/10.1038/s41560-023-01341-5.
[39] Monitoring report 2025 - Developments in the electricity and gas market. Bundesnetzagentur für Elektrizität, Gas, Telekommunikation, Post und Eisenbahnen; 2025.
[40] Germany 2025. International Energy Agency; 2025.
[41] Güntner J, Reif M, Wolters M. Sudden stop: Supply and demand shocks in the German natural gas market. J Appl Econom 2024;39:1282–300. https://doi.org/10.1002/jae.3089.